Influence of Pb(II) on the Radical Properties of Humic Substances and Model Compounds

E. Giannakopoulos,[†] K. C. Christoforidis,[†,‡] A. Tsipis,[§] M. Jerzykiewicz,*[,∥] and Y. Deligiannakis*[,†]

Laboratory of Physical Chemistry, Department of Environmental and Natural Resources Management, University of Ioannina, Seferi 2, 30100 Agrinio, Greece, Section de Bioenergetique, DSV, Commisariat al l'Energie Atomique Saclay, 91191 Gif-Sur-Yvette, France, Section of Inorganic Chemistry, Department of Chemistry, University of Ioannina, Panepistimioupolh Ioannina, Greece, and Faculty of Chemistry, Wroclaw University, 14 F. Joliot-Curie Street, 50-383 Wroclaw, Poland

Received: October 26, 2004; In Final Form: December 19, 2004

The influence of Pb(II) ions on the properties of the free radicals formed in humic acids and fulvic acids was investigated by electron paramagnetic resonance spectroscopy. It is shown that, in both humic acid and fulvic acid, Pb(II) ions shift the radical formation equilibrium by increasing the concentration of stable radicals. Moreover, in both humic acid and fulvic acid, Pb(II) ions cause a characteristic lowering of the stable radicals' *g*-values to $g = 2.0010$, which is below the free electron *g*-value. This effect is unique for Pb ions and is not observed with other dications. Gallic acid (3,4,5-trihydroxybenzoic acid) and tannic acid are shown to be appropriate models for the free radical properties, i.e., *g*-values, Pb effect, pH dependence, of humic and fulvic acid, respectively. On the basis of density functional theory calculations for the model system (gallic acid−Pb), the observed characteristic *g*-value reduction upon Pb binding is attributed to the delocalization of the unpaired spin density onto the Pb atom. The present data reveal a novel environmental role of Pb(II) ions on the formation and stabilization of free radicals in natural organic matter.

1. Introduction

Humic substances, which are the most widespread organic constituents of natural soils, are responsible for some of the most important environmental properties of soils.[1,2] Humic substances, together with clays and metal oxides, are the key factors determining the metal binding in soils.[1,3] Although no crystal structure of humic substances is available, spectroscopic and analytical data provide evidence that humic acids consist of several major functional groups, predominantly carboxylic (R−COOH) and phenolic (R−OH), as well as carbonyl (C═O), quinonoid, and alcoholic (OH).[1,4] Humic substances of any origin and nature are known to contain stable organic free radicals, which are indigenous to their structure and can be studied by electron paramagnetic resonance (EPR) spectroscopy.[5,6] The equilibria between structural polyphenolic and quinonoid units result in semiquinonoid radicals.[5,6] These stable radicals are considered to be involved in important chemical, biochemical, and photochemical processes occurring in soil and water systems.[7−13]

Interactions of humic substances with metal ions, such as Ca^{2+}, Zn^{2+}, Mg^{2+}, or Cd^{2+}, play a significant role in shifting the free radical reactions equillibria.[14−17] The effect of metal binding is observed as a change in the free radicals' EPR spectral intensity.[14−17] Recently, an EPR study showed that Pb(II) also influences the radical properties of humic substances.[18] Noteworthy, the effect of Pb(II) differs from other divalent cations' effect. EPR spectroscopy showed that the interaction of Pb(II) with humic acids results in the formation of new radicals, with a striking feature being their unusually low *g*-values, i.e., below the free electron *g*-value.[18] However no explanation or detailed analysis of the observed Pb(II) effect has been provided. Given the importance of Pb(II) in environmental physical chemistry,[1,19−22] this effect of Pb(II) may have important implications in the free radical chemistry of humic substances. Thus, connecting Pb(II) binding with the free radical chemistry of humics provides novel information on their behavior under real conditions.

In reference 18 a phenomenological correlation between the formation of the low *g*-value radicals and the amount of Pb bound in humic acid (HA) was established for powder samples. Furthermore FTIR spectroscopy provided evidence that the Pb(II)−HA radical is related with the interaction of Pb(II) ions with carboxy moieties in the humics.[18] However, due to the complex nature of humics, the structural units responsible for the stable free radicals could not be unequivocally identified. The structure of Pb(II) complexes with humic substances and catechol has been previously investigated using X-ray absorption spectroscopy,[21,22] but these results do not account for the formation of free radicals.

Given the complex nature of humics, an approach toward better understanding of their structure and interactions is to use low molecular weight model compounds with well-known physicochemical properties. In this approach, the use of carboxylic and/or aromatic molecules has already provided important insight in the spectroscopic[23,24] and structural properties of humic acids[25] and their interactions with oxide particles[26−28] and clays.[29] In the cited cases, successful models were organic molecules bearing one, or more, carboxy groups and/or phenolic or aromatic ring(s). The choice of these model molecules

* To whom correspondence should be addressed. E-mai: (Y.D.) ideligia@cc.uoi.gr; (M.J.) mariaj@wchuwr.chem.uni.wroc.pl.
[†] Department of Environmental and Natural Resources Management, University of Ioannina.
[‡] Commisariat al l'Energie Atomique Saclay.
[§] Department of Chemistry, University of Ioannina.
[∥] Wroclaw University.

10.1021/jp045121q CCC: $30.25
Published on Web 02/17/2005

stemmed largely from the evidence that humic acids consist mainly of carboxy and phenolic moieties.[1,2,30] To date, however, an analogous detailed investigation on models of the free radical properties of humic acids, i.e., their EPR characteristics and pH dependence, has not been reported. Published EPR spectral data refer to humic and fulvic acids,[5,7,14−17,31−35] which usually give an unstructured derivative. In scarce exceptions[34,35] hyperfine splittings have been resolved. Model molecules suggested to be responsible for quinoid radicals are benzoquinone,[5,7,34] methoxybezene radicals,[6,36] or N-associated radicals.[6] The existence of aromatic network conjugated to the semiquinone moiety has been speculated to be the origin of low *g*-values, i.e., via the delocalization of the electron spin density from the O atom(s) to aromatic C atoms through the aromatic network. [6,31] An interesting observation was made by Wilson and Weber,[36] who based on pH-dependent EPR data on fulvic acid concluded that a group of closely related semiquinone species, and not a single entity, was responsible for the free radical variation with pH. In summary, in the existing published works on EPR of humic and fulvic acids there is a lack of a detailed investigation, at a molecular and electronic level, of the radical properties by appropriate model compounds.

Thus, our approach was to search for pertinent model molecules which (a) will reproduce the spectral, i.e., EPR, and physicochemical properties, i.e., such as stability and pH dependence, of the stable radicals in humics and (b) will reproduce the observed effect of Pb(II) ions on the EPR spectra.

Pertinent information on the effects of diamagnetic metal ions on organic radicals can be found in previous works[37,38] where complexation of various metal dications with catechol was studied using EPR spectroscopy. However, Pb(II) was not included in these experiments. In the present case, we have focused our work on molecules bearing both carboxy and phenolic moieties. Among the widely accepted current theories for the humic substance formation is the "polyphenol theory": [1,2,4] According to this theory the major building blocks of humic substances originate from polyphenols of lignin origin or synthesized by microorganisms. In this model, *p*-hydroxybenzoic acid, protocatechuic acid (3,4-dihydroxybenzoic acid), and gallic acid (3,4,5-trihydroxybenzoic acid) are among the main low molecular weight aromatic acids formed after lignin degradation.[2,12,13] Subsequent polymerization of the mono-, di-, and trihydroxyphenolic compounds may occur in alkaline media, i.e., under conditions where radicals are formed, or alternatively operated by polyphenoloxidase enzymes.[12,13a] A number of published data, based on alkali metal degradation of humic acids, provides evidence that mono-, di-, and trihydroxy derivatives of benzoic acid are frequently among the structural units building humic acids.[13b]

Furthermore phenolic acids, such as tannic, *p*-hydroxybenzoic, protocatechuic, and gallic acids, and their esters are common plant constituents that are known for their antioxidant activities.[39,40] Gallic acid, which is a well-known antioxidant, is a common pollutant in oil refineries,[43] and it is to be expected that its interaction with Pb ions should be considered as quite possible for example in metal contaminated oil refinery sludges.

The radical scavenging abilities of these phenolic acids depend greatly on the number and arrangement of phenolic hydroxyl groups. Thus, it has been documented that gallic acid possesses a higher radical scavenging activity than protocatechuic acid, whereas 4-hydroxybenzoic acid shows little radical scavenging activity.[40−43] Hence, pyrogallol-type triphenols carrying three adjacent hydroxyl groups on a benzene ring effectively scavenge more radicals than catechol-type *o*-diphenols.[42,43]

In this context we have carried out a systematic investigation on the EPR characteristics and of pH dependence several hydroxybenzoic acids bearing one carboxy and either one-, two-, or three OH groups. For completeness we have also investigated tannin, tannic acid, chitosan, *p*-benzoquinone, phenol, and catechol. Subsequently we have investigated the effect of Pb(II) on the spectral properties and the pH dependence of radicals formed under autoxidation of these molecules. Our data show that among them, gallic acid (3,4,5-trihydroxybenzoic acid) gives radicals whose properties resemble most closely the properties of stable radicals in humic acids. Accordingly we have carried out a more detailed study of the gallic acid radical and its interaction with Pb(II). In addition to experimental data, we have carried out theoretical (density functional theory (DFT)) investigation of the formation and properties of the new radicals. Density functional theory has been proven to be an accurate predictive tool not only for the calculation of molecular geometries but also for the computation of physical and spectroscopic properties of molecules such as NMR shifts, hyperfine and dipolar coupling constants, and nuclear quadrupolar couplings.[44] Theoretical calculation of **g**-tensors needs further improvement,[44] although considerable progress is been achieved in this field.[45−47] Recently theoretical calculations for gallic acid and other phenolic compounds provided theoretical foundation of their vibrational spectroscopic characteristics[48] as well as on the mechanism of their antioxidant activity.[49]

In this paper, we have used DFT with the following objective: (i) to determine the structures and properties of the respective complexes of Pb(II), (ii) to explore the role of Pb(II) ions in the radical formation process, and (iii) to set limits on the minimal requirements of organic molecules that can act as building blocks of humic acids in terms of radical formation and behavior under certain characteristic conditions such as Pb binding. The DFT calculations focus on the stabilization energies of the formed compounds and the spin density distributions.

2. Experimental Section

Humic and fulvic acids (HA and FA) were extracted from different sources: (1) compost HA and FA from compost produced by the Municipal Composting Plant in Zabrze (Upper Silesia, Poland); (2) peat HA and FA from low moor peat (Odra river lowland near Wroclaw, Poland). The isolations were carried out using standard IHSS (International Humic Substances Society) procedure[2,50,51] by shaking the compost samples in a solution of NaOH and $Na_4P_2O_7$ and centrifugation and acidification to pH 1.0 with HCl. Fulvic acids were purified using XAD-8 and AG-MP 50 resins.

Tannin, tannic acid, chitosan (low and high molecular weight), aluminon, gallic acid (3,4,5-trihydroxybenzoic acid, 3,4,5-thb, GAH_4), 2,4,6-trihydroxybenzoic acid (2,4,6-thb), and 2,3-dihydroxybenzoic were purchased from Aldrich. Metal ion solutions were prepared by using $Pb(NO_3)_2$, $Zn(NO_3)_2$, $Mg(NO_3)_2$, $Cb(NO_3)_2$, or $Pb(CH_3COO)_2$ from Aldrich.

Solid State Studies. To obtain the powder complexes with Pb(II), the humic acids, tannin, tannic acid, chitosan, and aluninion (0.5 g) were treated with 15 mL of 0.03 M lead acetate. Fulvic acids, gallic acid, 2,4,6-thb, 2,3-dhb, 2,4-dhb, 2,5-dhb, 2,6-dhb, 3,4-dhb, 3,5-dhb, salicylic acid, and catechol were previously dissolved and mixed with 15 mL of 0.03 M lead acetate. The purified and dry powders containing the Pb(II) complexes were examined by spectroscopic and chemical methods. The effective amount of metal uptake was assessed

in each case by ICP spectroscopy. Solid-state, cross polarization, magic angle splitting (CP MAS) ^{13}C NMR spectra were measured on a 300 MHz Bruker spectrometer. The operating conditions were as follows: spinning rate, 4.6 kHz; contact time, 1ms; number of scans, 3000. Infrared spectra (IR) were recorded with a FT-IR Bruker 113v spectrometer on KBr pellets (1 mg sample in 400 mg of KBr).

Liquid-Phase Studies. Potentiometric titrations were performed with an automatic pH tritrator Metrohm Titrino900, equipped with a double-wall thermostated cell. The solution was under continuous stirring and exhaustive bubbling with ultrapure (99.999%) N_2 gas. All solutions were made in ultrapure Milli-Q water produced by a Millipore-Academic system. Before starting the titrations the solutions were bubbled exhaustively to remove dissolved CO_2. The pH titrations were performed in triplicate by adding a controlled amount of KOH solution in microliter doses. Theoretical analysis and simulation of the titration data were performed by using the program FITEQL.[52]

Electron Paramagnetic Resonance Spectroscopy. Continuous wave electron paramagnetic resonance spectra were recorded with either a Radiopan SE or a Bruker ESP300E spectrometer operating at X-band frequencies. Spectra were recorded at room temperature for powder samples or at cryogenic temperatures for liquid samples. The Bruker spectrometer with a 100 kHz magnetic field modulation was equipped with Bruker NMR gaussmeter ER 035M and Hewlett-Packard microwave frequency counter HP 5350B. A Li/LiF standard was used for *g*-value calibration; 4-hydroxy-TEMPO and Reckitt's ultramarine were used as standards of spin concentration.

The quantitative EPR technique (QEPR) was applied (microwave power, 2 mW; modulation amplitude, 1 G; 20.0 mg sample; standard quartz tubes; etc.). The standard peat and leonardite HA produced and distributed by IHSS were used as additional standards of free radical concentration. Simulation of the EPR spectra was performed by using the program WINEPR−SimFonia, version 1.25 by Bruker.

3. Theoretical Calculations

The structural, electronic, and energetic properties of all compounds were computed at the Becke's three-parameter hybrid functional[53] combined with the Lee−Yang−Parr[54] correlation functional termed as the B3LYP level of density functional theory using the SDD basis set, which describes valence electrons with a [8s,7p,6d/6s,5p,3d] valence basis set[55] and Stuttgart−Dresden relativistic ECP's. The Stuttgart relativistic pseudopotential uses the (4s,4p,1d)/[2s,2p,1d] basis with a [3,1] contraction scheme for third- and fourth-row atoms.[56] Recently it was found that the B3LYP/SDD approach provides a good compromise between accuracy and computational cost for Pb-containing molecules.[57]

In all computations no constraints were imposed on the geometry. Full geometry optimization was performed for each structure using Schlegel's analytical gradient method,[58] and the attainment of the energy minimum was verified by calculating the vibrational frequencies that result in the absence of imaginary eigenvalues. All the stationary points have been identified for minimum (number of imaginary frequencies NIMAG = 0) or transition states (NIMAG = 1). The Mulliken net atomic charges, bond overlap populations (bop), and atomic spin densities were obtained by employing Mulliken population analysis,[59] while the natural bond orbital (NBO) method, developed by Weinhold et al.,[60] was employed in order to obtain the natural charges on the atoms. All calculations were performed using the GAUSSIAN03 series of programs.[61]

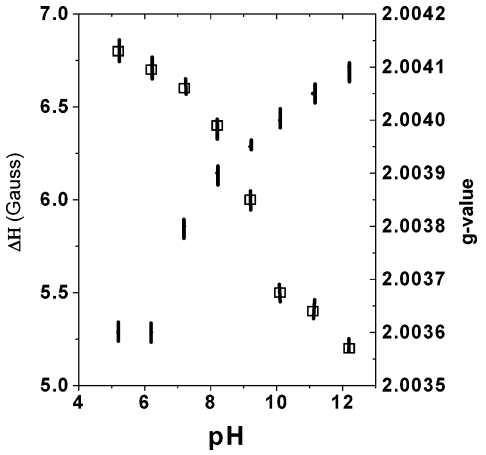

Figure 1. Electron paramagnetic resonance (EPR) line width (open squares) and *g*-values (dots) for humic acid solutions at various pH values. The bars indicate the variation of the corresponding parameters based on data from three different sources of humic acid. EPR conditions: microwave power, 1.25 μW; modulation amplitude, 1.0 Gpp; modulation frequency, 100 kHz; microwave frequency, 9.42 GHz; temperature, 30 K.

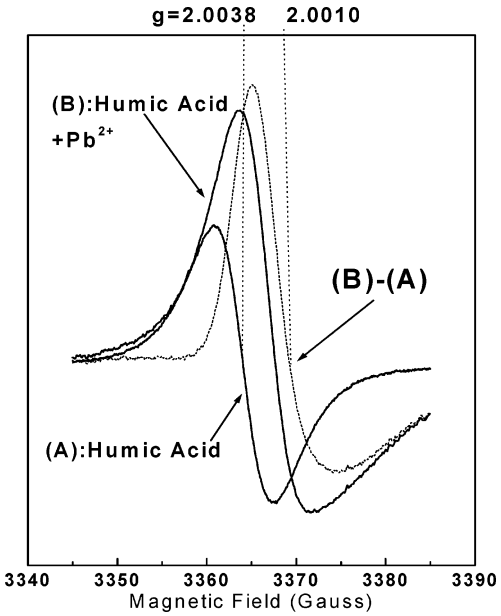

Figure 2. EPR spectra for humic acid (trace A) and humic acid−Pb(II) (trace B). Both samples are at pH 6.8. The humic acid−Pb sample was incubated at 25 °C for 6 h. The dotted line is a numerical subtraction of spectrum A from spectrum B. The vertical dotted line is a guide to the eye to visualize the *g*-value shift upon interaction with Pb. EPR conditions as in Figure 1.

4. Results and Discussion

(4.1) Formation of Low-*g* Radicals upon Interaction with Pb^{2+}. *Pb−Humic Acid.* The EPR signal of untreated powder humic acid is a singlet radical with a *g*-value of 2.0034 and $\Delta H = 6.7$ G. In solution, the EPR signal (line width and *g*-value) depends strongly on pH; see Figure 1. A typical signal for humic acid at pH 6.8 is displayed in Figure 2, signal A. The EPR signal intensity increases monotonically on going toward alkaline pH values. These EPR characteristics are typical for humic acids and are in agreement with literature data values.[5,6,14−18]

Incubation of humic acid solution with Pb at pH 6.8 results in characteristic modification of the EPR signal; see signal B

in Figure 2. Signal B has a lower *g*-value than signal A with a concomitant increase in its overall intensity. A computer subtraction of the EPR signal A from B (see dotted signal in Figure 2) shows that signal B contains a large radical with a *g*-value near 2.0010, i.e., below the free electron *g*-value. This effect of Pb has been originally reported for freeze-dried humic acids treated with Pb.[18] Here we show that the Pb effect takes place in solution also.

A detailed study of the *g*-shift reveals that the limiting value of $g = 2.001$ is attained only after a long incubation time of humic acid and Pb, i.e., at least 6 h. From these observations we conclude that the Pb(II) ions interact with a fraction of the radical sites in HA and give the $g = 2.0010$ radicals. Moreover the long incubation time required suggests that these radicals are located at sites not immediately accessible by the solution ions, i.e., at the interior of the humic polymeric matrix.

Pb−Fulvic Acid. Untreated fulvic acid does not gives EPR radical signals, neither in solution nor in freeze-dried powder samples (data not shown). In contrast, after incubation with Pb(II) a stable radical is formed in FA−Pb(II) as it is evidenced by the EPR spectrum which is quite similar ($g = 2.0013$; $\Delta H = 13.5$ G) to that displayed in Figure 2, for [humic acid−Pb].

In summary, the present data demonstrate that (a) Pb(II) ions increase the amount of stable radicals in humic acid while they induce the formation and stabilization of radicals in fulvic acid. (b) the radicals formed in the presence of Pb(II) ions have a characteristic low *g*-value near 2.0010, which is well below the free electron *g*-value of 2.0023. The observation of the induction of significant *g*-shift in the EPR radical signals of humic acid is a novel finding which deserves deeper analysis.

Pb(II) is a diamagnetic metal, and no other oxidation states, i.e., other than 2+, are expected under our experimental conditions. At pH 6.8, e.g., for the samples giving the spectra in Figure 2, hydrolysis of Pb is prevented since the p*K* of $Pb(OH)^+$ formation is at 7.7.[62] This indicates that the species involved in the *g*-shift are the Pb^{2+} ions rather than $Pb(OH)^+$ or other Pb−hydroxide species. To see if the observed Pb effect is solely due to its positive charge, we have tested other dications as well, i.e., Cd^{2+}, Zn^{2+}, Mg^{2+}, and Ca^{2+}. In the samples of humic acid and fulvic acid, as well as in the model compounds that we discuss in the following, these cations have no effect on the *g*-value of the EPR radical signal. In accordance with previous observations in freeze-dried powder samples of humic acid,[17] in solution samples these dications cause an increase in the radical signal intensity. Thus the effect of Pb ions on the *g*-value shift appears to be unique.

Given the complicated and yet unknown structures of humic and fulvic acids, we have carried out a systematic search for pertinent low molecular weight model compounds for the free radical properties of humic and fulvic acids.

EPR on Model Molecules. For the sake of the presentation we group the used model molecules in two families. One family of model molecules was simple phenolic acids; see Chart 1. In the second family of molecules we have examined more complex polyphenolic molecules such as chitin, chitosan, alumininon, tannin, and tannic acid. Our EPR experiments on the radical formation under O_2 oxidation show that among the tested molecules only gallic acid, tannin, and tannic acid give EPR radical signals after interaction with Pb(II) ions. The EPR signals from tannin and tannic acid, are comparable to the EPR parameters for the signals obtained from fulvic acid; see Table 1. From Table 1 we see that, the highest free radical concentration is observed for tannic acid and tannin−Pb(II) complexes (7×10^{18} and 6.3×10^{18} spins/g). The stability of the radicals

CHART 1

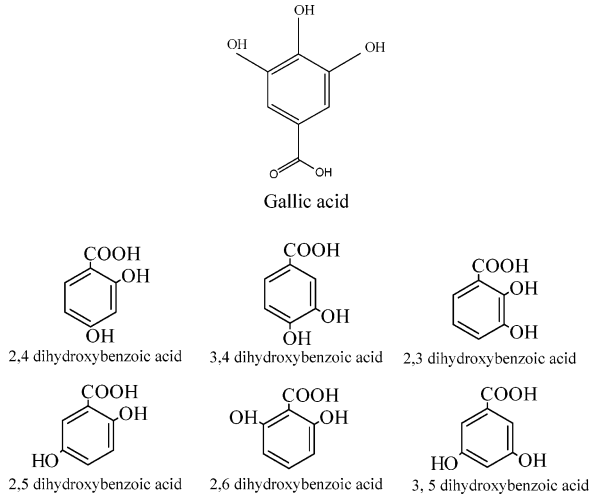

TABLE 1: *g*-Value and Spin Concentration in Powder Humic, Fulvic, Dihydroxybenzoic, and Gallic Acids Complexed with Pb(II)

	spin concn × 10^{-18} (spins/g)	*g*-value[a]	Pb(II) concn (mmol/g)
humic acid−Pb(II)	2.3	2.0010	1.23
fulvic acid−Pb(II)	0.18	2.0013	1.81
tannin−Pb(II)	6.3	2.0013	2.06
tannic acid−Pb(II)	7.0	2.0013	2.10
gallic acid−Pb(II)	0.19	2.0010	2.34
catechol−Pb(II)	no signal		2.61
2,3-dihydroxybenzoic acid−Pb(II)	0.16	2.0010	2.91
3,4-dihydroxybenzoic acid−Pb(II)	0.02	2.0011	2.7

[a] Error: ±0.0002.

in tannic acid and tannin−Pb(II) complexes can be attributed to their structure, i.e., stabilization of the radicals through delocalization over the ring orbitals. The EPR signals from gallic acid in the presence of Pb are comparable to the new radical formed in the HA−Pb sample. In light of these observations we thought it would be advisable to look for compounds simpler than gallic acid, which are also considered to be constituents of humic substances,[13b] namely, the isomeric dihydroxybenzoic acids (dhb; Chart 1). Among them, after interacting with Pb(II) we were able to obtain EPR radical signals only for 3,4-dhb and 2,3-dhb. It is noticed that these are the only two molecules having adjacent OH moieties. All the other isomeric dihydroxybenzoic acids, involving no adjacent OH groups (2,5-dhb and 2,6-dhb, etc.), do not give detectable stable EPR signals. The same holds also true for 4-hydroxybenzoic acid, salicylic acid, phenol, or catechol, which after incubation with Pb(II) ions don't give any EPR signal. In the case of *p*-benzoquinone, at alkaline pH under O_2 oxidation we obtain the familiar EPR signals; i.e., $g = 2.0044$ and $\Delta H = 9.5$ G.[63] This signal remained unaltered in the presence of Pb(II) ions.

In summary the present data show that among the studied model compounds, only molecules such as protocatechuic acid (3,4-dihydroxybenzoic acid) its isomeric structure 2,3-dihydroxybenzoic acid and gallic acid (2,4,6-trihydroxybenzoic acid) result in the formation of stable radicals after complexation with Pb(II) ions. These data lead to the following suggestions: (a) the relative position of the OH groups is of key importance in the formation of the new radicals upon complexation with Pb(II). OH groups in vicinal positions are necessary for the new

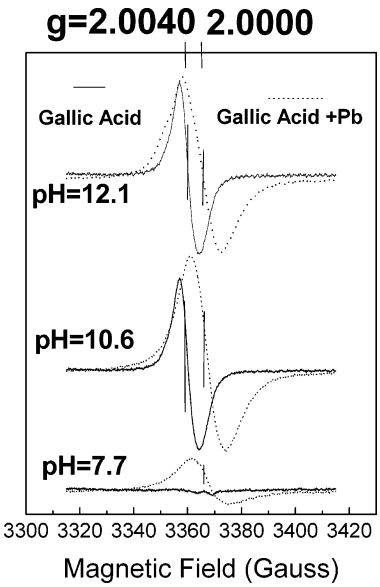

Figure 3. Low-temperature EPR spectra for gallic acid (solid lines) and gallic acid−Pb (dotted lines) as a function of pH. The samples were prepared with equimolar concentrations of gallic acid and Pb, incubated for 40 min at pH 6.0, and then the pH was raised to the indicated value, where it was exposed to ambient O_2 by air-bubbling for 15 min at 25 °C. Temperature, 28 K. Other EPR conditions as in Figure 1.

radicals to be formed; (b) molecules bearing only one OH group do not form radicals upon interaction with Pb(II); (c) the experiments with catechol and *p*-benzoquinone show that the carboxy group is also required for the formation of the low *g*-value radical in the presence of Pb.

In the following, we have carried out a more detailed pH dependence of the radicals observed in Pb−humic acid and Pb−gallic acid, with the aim being to study the structural and electronic properties of the complex in correlation with its unusual EPR signal, i.e., the *g*-value. Furthermore, understanding the properties of gallic acid is of more general interest due to its widely acknowledged andioxidant and radical scavenging role.

pH Dependence of Gallic Acid Radicals. Figure 3, solid lines, presents frozen solution EPR spectra for gallic acid (GA) at various pH values after exposure to ambient oxygen for 15 min. At acidic or neutral pH values, pH < 8, no EPR signal is detected. On going to alkaline pH values, we detect a singlet EPR signal in the $g = 2$ region. The signal has a slightly pH-dependent *g*-value; i.e., *g* varies between 2.0039 and 40. At pH 10.6, under nonsaturating EPR conditions, the line width in the frozen solution samples is $\Delta H = 6.8$ G, while at pH 12.1 the signal is narrower, $\Delta H = 5.6$ G.[66]

pH Dependence of Pb−Gallic Acid Radicals. Figure 3, dotted lines, presents EPR spectra of gallic acid solutions in the presence of an equimolar amount of $Pb(NO_3)_2$. The Pb−GA samples were treated in exactly the same way as the GA samples giving the EPR signals in Figure 3. A striking observation is the significant shift by ∼7.0 G in the Pb−GA samples. The shifted *g*-value, corresponding to $g = 2.0010$, in Figure 3 is quite similar to that observed in Figure 2 for humic acid−Pb (see signal B in Figure 2). This *g*-shift in the gallic acid−Pb samples is observed at all pH values where EPR signals are detected; see Figure 3. A detailed comparison of the EPR signal intensities as a function of pH, see Figure 4, reveals a shift in the pH profile of the Pb−GA EPR signals. According to Figure 4, in the case of gallic acid alone we can detect radical signals

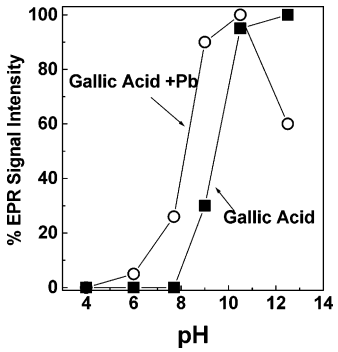

Figure 4. Double integral of the EPR spectra for gallic acid (solid squares) and gallic acid−Pb (open circles) as a function of pH. The samples were prepared with the same protocol as in Figure 3. For each sample the EPR integral was normalized to the maximum signal observed, i.e., pH 12 for gallic acid and pH 10.4 for gallic acid−Pb. Temperature, 28 K. Other EPR conditions as in Figure 1.

only at pH > 8, while in the Pb−GA sample stable radicals are formed at near-neutral pH values, even at pH 6. Thus, Pb interaction with GA results in an enhancement of radical stabilization at lower pH values. A similar enhancement of the radical signals is observed in humic acid and fulvic acid in the presence of Pb ions. A computer deconvolution of the EPR signal of the Pb−GA sample at pH 12.1 shows that it contains a significant amount, i.e., 40% from the GA/pH 12 EPR signal. As we show in the following, all these differences on the pH profiles of the EPR signals of the two samples can be attributed to pK_a shifts induced by Pb complexation with GA. Before that we discuss some spectroscopic data which will assist in the structural assignment of the reacting species.

(4.2) FTIR Study of the Structure of the Pb(II) Complexes. The FTIR spectra for Pb(II) complexed with humic acid and fulvic acid show changes in stretching frequencies of carboxyl groups (1635−1700 cm^{-1});[67] see Figure S1-A of the Supporting Information. In the presence of Pb(II) these absorbances change to one unresolved band shifted to lower wavenumbers (1520−1600 cm^{-1}).[18] For dihydroxybenzoic acids, the band of ν(C−O) at 1230−1300 cm^{-1} observed in the FTIR of pure acids shifts to the values around 1380 cm^{-1} upon complexation with Pb(II); see Figure S1-V of the Supporting Information. According to Nakamoto, the value of the parameter Δ (calculated as $\Delta = \nu(C{=}O) - \nu(C{-}O)$) in the range $\Delta = 120{-}160$ cm^{-1} indicates formation of bidentate complexes.[68] The existence of unidentate ($\Delta = 250{-}300$ cm^{-1}) complexes is also possible. However, the limited resolution of our FTIR spectra in the range of 1200−1290 cm^{-1} does not allow a positive confirmation of this possibility. Binding of Pb(II) ions through the carboxyl group is further evidenced by changes observed in the broad band at ∼3000 cm^{-1}, which can be attributed to a carboxyl group intermolecular hydrogen bond.[69,70] In the cases of dihydroxybenzoic acids, complexation with Pb(II) results in disappearance of this broad band (see Figure S1-B of the Supporting Information). This may be taken as evidence of the reaction of the carboxyl group with the metal ion. Similar spectral changes and analogous interpretation are valid for 2,3-dhb and its Pb(II) complex spectra (see Figure S1-B of the Supporting Information).

Complexation of gallic acid with the Pb cations at different molar ratios gives FTIR spectra which indicate reaction of Pb with the carboxyl group (Figure S2 of the Supporting Information). The broad band at 3287 cm^{-1} observed in the spectrum of the pristine gallic acid is attributed to OH stretching vibrations ($O_{14}H_{15}$) of the carboxyl groups, while the bands at 3496 and 3422 cm^{-1} correspond to OH stretching vibrations of the

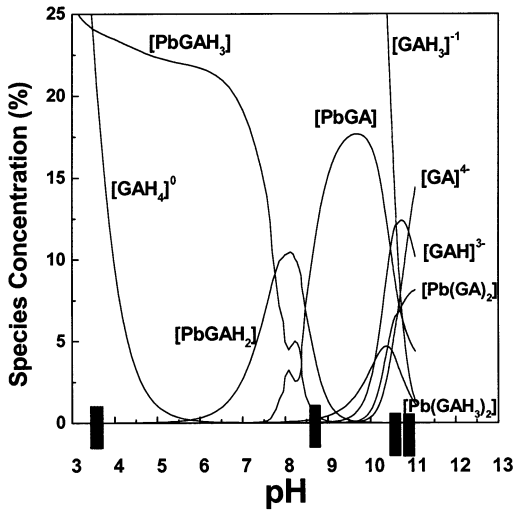

Figure 5. pH dependence of the species distribution for gallic acid−Pb obtained by fitting pH−titration data. The thick bars at the pH axis indicate the pK_a values used in the fit, which are reported in Table 2. The stability constants used in the fit are reported in Table 2.

phenolic groups O_9H_{16} and $O_{10}H_{17}$, respectively.[71] The band at 3063 cm^{-1} is due to C−H stretching vibrations (C_2H_8 and C_6H_{12}), whereas the absorption at 3368 cm^{-1} originates from vibrations of absorbed water molecules in the KBr matrix.[71] From the above bands the one at 3287 cm^{-1} seems to be more affected from the reaction with lead cations. As the Pb^{2+}/gallic ratio is increased, the band is gradually shifted to lower wavenumbers (3249 cm^{-1}), indicating that gallic acid molecules bind lead(II) mostly through the carboxylic group. A small shift is also observed for the O_9H_{16} vibration (from 3496 to 3478 cm^{-1}), indicating that the phenolic group in the meta position may also take part in complex formation with Pb(II), while all the other bands in this region seem to be unaffected by this complexation. The above findings are in agreement with the studies of Vicedomini[72] on the complexation equilibria between gallic acid and Pb(II) which support the formation of a 1:1 complex between the cation and the carboxylic group of the ligand. Analogous complexation behavior was also observed for gallic acid when this was treated in aqueous solution with aluminum(III) cations.[73,74]

(4.3) CP MAS ^{13}C NMR. The CP MAS ^{13}C NMR spectra of HA, FA and HA−Pb(II), FA−Pb(II) are typical for these substances[75] and do not show significant differences. The only noticeable difference concerns the broadening of the carboxyl groups band, as a result of the formation of the HA−Pb(II) and FA−Pb(II) complexes. In the case of gallic acid−Pb(II) and 2,3-dhb−Pb complexes (Figure S3 of the Supporting Information), the ^{13}C NMR lines of the carboxy carbon are shifted, while the peaks of the O-substituted aromatic carbon (2 and 3 in Figure S3 of the Supporting Information) disappear after reaction with the Pb ions. In addition the aromatic carbon peaks merge into one unresolved peak. These changes show that complexation of Pb with gallic acid or 2,3-dhb acid results in redistribution of the electron density in the ring. This is corroborated by our DFT calculations that we will discuss in the following.

(4.4) pH Speciation of Gallic Acid and Pb−Gallic Acid. The formation of stable radicals at alkaline pH due to oxidation by O_2 is a well-documented phenomenon for quinones and phenolic compounds[63]

$$R-OH \xrightarrow{pH>9} R-O^- \xrightarrow{O_2} R-O\bullet \qquad (1)$$

The formation of stable gallic acid radical via O_2 oxidation under

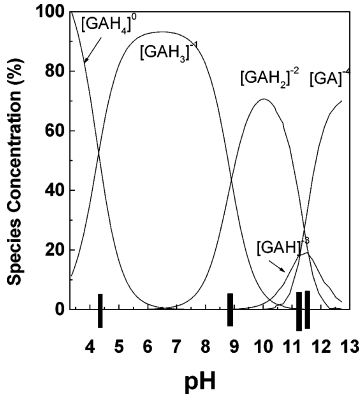

Figure 6. pH dependence of the species distribution for gallic acid obtained by fitting pH−titration data. The thick bars at the pH axis indicate the pK_a values used in the fit, which are reported in Table 2.

TABLE 2: Equilibrium Constants (pK_a and K) for Gallic Acid Complexed with Pb(II)

	pK_a[a]	species	equilib const, log K[b]
gallic acid	4.3, 8.8, 11.4, 11.7		
		Pb−GAH_3	8.5
		Pb−GAH_2	9.0
gallic acid−Pb(II)	3.6, 8.9, 10.8, 11.2	Pb−GAH	7.0
		Pb−GA	11.9
		Pb−$(GA)_2$	14.4

[a] Error: ±0.1. [b] Error: log K, ±0.5.

alkaline conditions is well-documented[65,76] as well. However, no detailed pH dependence and speciation analysis of the molecular origin of the gallic acid radicals has been reported. The pH dependence of the formed radicals for gallic acid, is displayed in Figure 3 (solid squares). As we show in the following, the interaction with Pb(II) shifts the pH dependence of the radical formation, e.g., see Figure 3 (open squares), due to shifts in the pK_a values of the ring OH groups.

The pH titration of 1:1 gallic acid/Pb(II) (Figure S4 of the Supporting Information) reveals a significant change on the proton release properties of gallic acid, due to the presence of the Pb(II) ions. At acidic pH values, <pH 4, a significant amount of protons are released from gallic acid due to Pb. As we demonstrate by the theoretical simulation of the pH-titration curve (see continuous line in Figure S4 of the Supporting Information), this H-release is due to a pH shift in the carboxy proton of gallic acid. Thus, in accordance with the FTIR data, at acidic pH the Pb(II) ions interact with gallic acid, forming complexes via the carboxy oxygen. Based on the fit of the pH titration data, the speciation analysis for gallic acid (Figure 6) and gallic acid−Pb (Figure 5) shows that at pH > 4 a significant fraction of monoioninic gallic acid is complexed with Pb(II), i.e., forming a $PbGAH_3$ complex. In the absence of Pb(II) the monoionic gallic acid $[GAH_3]^{-1}$ is the dominant species in the range of pH 4−8; see Figure 5. The pK_a values of the four protons of gallic acid, listed in Table 2, are 4.3, 8.8, 11.4, and 11.7 in accordance with the reported values.[77] For the sake of the discussion these pK_a values are marked by the thick black bars in the pH axes in Figures 5 and 6. From Table 2 we see that complexation with Pb induces pK_a shift in the gallic acid's protons. The pK_a of the carboxy proton is shifted to pK_a = 3.6 in the gallic acid−Pb(II) complex. At the alkaline pH edge the two, nearly equivalent, pK_a values of the ring OH's of gallic acid (pK_a = 11.7 and 11.4, respectively) are shifted to 10.8 and 11.2, respectively, upon Pb(II) complexation. The pK_a of the other ring OH (pK_a = 8.8 in gallic acid) is less affectd by Pb-

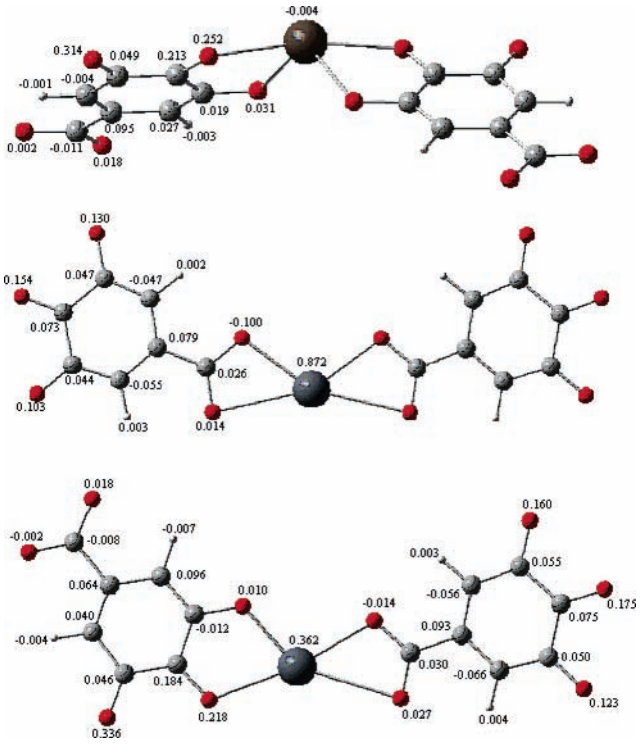

Figure 7. Equilibrium geometries and spin density isosurfaces (0.002 au) of the 1:2 complexes of Pb(II) with the gallic acid radical trianion, $[GA]^{3-\bullet}$, computed at the B3LYP/SDD level.

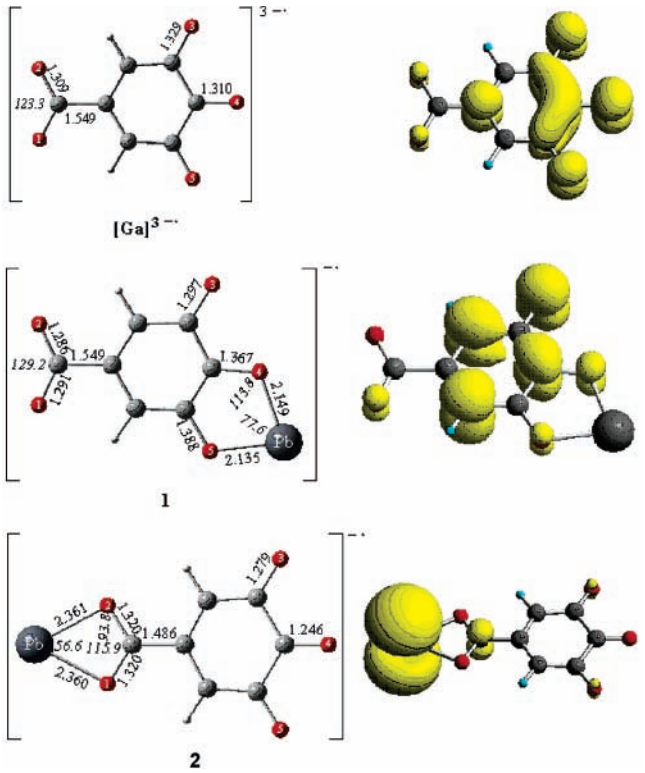

Figure 8. Equilibrium geometries and spin density isosurfaces (0.002 au) of the 1:1 complexes of Pb(II) with the gallic acid radical trianion, $[GA]^{3-\bullet}$, computed at the B3LYP/SDD level.

(II), i.e., becomes $pK_a = 8.9$ in gallic acid−Pb(II). From Figure 6, we see that, in the sample with equimolar concentrations of Pb and GA, the formation of 1:2 Pb/GA species appears to play a secondary role.

(4.5) Computational Studies Using DFT. *Equilibrium Geometries, Electronic Structure, and Bonding Mechanism in Pb(II)−Gallic Acid Complexes.* On the basis of the spectroscopic data and the speciation analysis and in order to keep the discussion at a tractable level, among the numerous species and their possible combinations with Pb(II), we have investigated the energetics of formation of two kinds of complexes; i.e., Pb/GA = 1:1 or Pb/GA = 1:2. The equilibrium structures along with selected structural parameters are depicted schematically in Figures S5 and S6 of the Supporting Information. The DFT calculations reveal the role played by the details of the coordination mode of the $[GA]^{3-\bullet}$ ligand with respect to the accumulation of the spin density on the central Pb(II) ion.

DFT on 1:1 GA/Pb Complexes. According to the calculations the free $[GA]^{4-}$ is calculated to be planar with C_{2v} symmetry. The loss of energy due to the formation of the radical is balanced by the stabilization gained from resonance in the aromatic π system. In the ambident $[GA]^{3-\bullet}$ anion there are five electron-rich binding sites (the five O donor atoms); thereby it could be coordinated to Pb^{2+} cation according to the following bonding modes: (i) through the O donor atoms of the carboxylato group either in a monodentate or a bidentate coordination mode and (ii) through the adjacent phenolate O donor atoms in a bidentate bonding mode forming a five-membered chelate ring. Moreover, the 1:1 and 1:2 gallic acid complexes of Pb(II) have been considered; see Figure 7. The ligand dissociation energies in isomers **1** and **2** were calculated to be 692.3 and 675.8 kcal/mol, respectively. Thus, coordination of Pb(II) to the phenolate O donor atoms, yielding complex **1**, is favored with respect to coordination to the carboxylato end (complex **2**) by about 16.5 kcal/mol. This is expected on the grounds of the higher stability of the five- versus four-membered chelate rings formed. The relatively high ligand dissociation energies illustrate that the metal−ligand bonding involves a strong electrostatic component since the interacting species have opposite charges. On the other hand, the covalent component of the bonding is higher in **1** than **2** is mirrored on the Pb−O bond lengths (see Figure 8). Attachment of the Pb^{2+} ion either to the carboxylato or the phenolato O donor atoms of the $[GA]^{3-\bullet}$ ligand leads to structural changes accompanied by significant charge redistributions as well. The structural changes, as it is expected, concern merely the coordination environment of Pb^{2+} (Figure 8). The Mulliken net atomic charges, natural charges, and bond overlap populations (bop) are given in Supporting Information (Table S1). There is a strong charge transfer from the coordinated $[GA]^{3-\bullet}$ ligand toward the central Pb(II) ion amounting to 0.92 and 1.33 charge units of natural charge in **1** and **2**, respectively. Although one would expect a higher charge transfer to occur in **1** as a result of the larger bop values of the Pb−O bonds (0.23 vs 0.11) the opposite is true.

Spin Densities. With regard to the EPR data it is of special interest to examine the influence of the Pb−GA coordination on the unpaired electron spin density distribution. In Figure 8 (right panels) the clouds help to visualize the unpaired spin density distribution. The numerical values of the spin density at each atom are displayed in Figure 8. Accordingly to the DFT data, in the absence of the Pb, the $[GA]^{3-\bullet}$ radical has the spin density mainly localized on the ring oxygens and on the ring carbons. The two ring protons bear only a small $^1H(I=1/2)$ fraction of the spin density, i.e., of the order of 0.5%. Such a small spin density corresponds to a small isotropic hyperfine coupling[64] which would result in a triplet $^1H(I=1/2)$ hyperfine structure. In fact such a triplet EPR spectrum can be detected in liquid gallic acid samples[65] at alkaline pH.

The DFT calculations predict that complexation of Pb with $[GA]^{3-\bullet}$ results in accumulation of the spin density on the central Pb(II) atom (spin density of 0.98|e| localized on a pure

6*pz* atomic orbital of Pb) in **2** as it is shown in Figure 7. In contrast, the spin density in **1** is primarily localized on the phenyl ring (total spin density of 0.86|e|) and the uncoordinated phenolic O atom (spin density of 0.44|e|). In both **1** and **2** the two ring protons bear a small fraction of the spin density. In **1** the calculated spin density of 0.1% corresponds to an Aiso(^{1}H) = 0.5 G,[64] which would result in an EPR spectrum with a triplet hyperfine splitting of 1.0 G; i.e., a narrowing of the EPR spectrum is predicted upon Pb complexation. In **2** the ^{1}H couplings increase and become nonequivalent, i.e., 9.5and 11.1 G. This would result in a significant broadening of the EPR spectrum, which is in accordance with the experimental spectra in Figure 3.

In summary the DFT calculations provide direct explanation for the spectral changes observed in the EPR signals of gallic acid interacting with Pb. The main conclusion is that the Pb ion is complexed via the carboxy oxygens and this allows a significant delocalization of the unpaired spin density onto the Pb atom, and this is the reason for the observed shift of the *g*-value upon Pb coordination. For comparison, we have carried out DFT calculations for the complex GA/Mg, which in the experimental data does not shift the *g*-value. The calculations (see Figure S7 of the Supporting Information) show that the delocalization of unpaired spin density onto the Mg atom is lemite, i.e., of the order of 14%. This is in acordance with the negligible change observed in the expiremental EPR spectrum of gallic acid radical in the presence of Mg^{2+}. Therefore Pb is the only cation inducing the charachteristic *g* lowering.

DFT for 2:1 GA/Pb Complexes. In addition to the 1:1 complexes, Pb(II) could also afford three possible isomeric 1:2 complexes, namely, complex **3** (Figure 7) involving coordination of the two $[GA]^{3-\bullet}$ ligands through the phenolate O donor atoms or complex **4** involving coordination of both $[GA]^{3-\bullet}$ ligands through the carboxylato groups or complex **5** involving coordination of one $[GA]^{3-\bullet}$ ligand through the phenolato and the other through the carboxylato groups. All three species are minima on the potential energy surface with complex **3** corresponding to the global minimum. Complex **3** adopts a "butterfly" structure with two short and two long Pb−O bonds. In this structure the spin density is localized on the two $[GA]^{3-\bullet}$ ligands with distribution analogous to that of the free $[GA]^{3-\bullet}$ ligand. Probably, the nonplanarity of the structure interrupts the conjugation, and therefore delocalization of spin density toward the Pb(II) central metal atom is not allowed (spin density of 0.00|e|). On the other hand, complex **4** being a local minimum at 30.2 kcal/mol higher in energy adopts a perfect planar structure (C_{2v} point group) with an asymmetric η^2-OOC bonding mode which supports the transfer of spin density to the central Pb(II) atom (spin density of 0.87|e|). Finally, isomer **5** located at 18.6 kcal/mol higher in energy than the global minimum adopts also a perfect planar structure with nonequivalent Pb−O bonds, where spin density delocalization toward Pb(II) could also be favored (spin density of 0.36|e|). Noteworthy in **5** is that spin density value on Pb(II) is nearly intermediate to those of isomers **3** and **4**.

The two ring proton spin densities in **3**−**5** become all nonequivalent. Moreover within the exception of one ring proton in **5** which bears 0.7% of the spin density, all other protons in **3**−**5** would bear smaller spin densities, i.e., smaller than the values in the free GA radical.

Considering that the isomeric species **3**−**5** dispose of open coordination sites, they could constitute the building blocks of polymeric structures. Such polymeric structures involving four-coordinated Pb(II) ions most likely take place in the powder samples and in solution in line with experiment. According to our calculations the purported polymeric structures should involve both modes of coordination of the gallic acid trianion, and therefore a fraction of the spin density could be located on the Pb(II) ion. This delocalization of the spin on Pb would deplete the C and O atoms from spin density, and this is the reason for the observed shift of the *g*-value detected in the EPR spectra. Obviously, the magnitute of the spin density on every Pb(II) ion in the polymer would be determined by the extent of participation of the carboxylato bonding mode of the $[GA]^{3-\bullet}$ ligand.

5. Conclusions

Complexation of Pb(II) with humic acids, fulvic acids, and other polyphenols results in the formation of the new radicals with unusually low *g*-values. For the low molecular weight polyphenols studied, the formation and stabilization of this radical is conditioned by the number and position of carboxylic and hydroxylic groups. Our data show that two or more hydroxyl groups in the nearest neighborhood are needed. Such arrangement can allow formation of stable chelating Pb(II) complexes. Gallic acid and tannic acid are good working models for the radical properties of humic acid and fulvic acid, respectively. For both humic and fulvic acid and the model compounds, the characteristic *g*-shift effect is unique for Pb ions and is not observed with other dications such as cadmium, magnesium, calcium, or zinc.

Environmental Implications. The DFT calculations revealed that spin density could be accumulated on the Pb(II) ion when the carboxylato bonding mode of the $[GA]^{3-\bullet}$ ligand is involved in the complex formation. This Pb coordination is manifested as a characteristic *g*-value shift to a limiting value of 2.0010. Therefore, in environmental soil organic matter samples the details of the Pb-complexation species could be predicted on the grounds of the amount of the spin density acquired by every Pb(II) ion, i.e., by the shift and the line shape of the EPR spectrum. The present data provide new insight for the application of EPR to detect Pb(II) polluted soils, peat, or composts. In addition the present data reveal that the interaction of humic and fulvic acids with Pb(II) facilitates stable radical formation. On the basis of model studies, i.e., on gallic acid, this is due to pK_a shifts induced on the hydroxyl protons upon interaction with Pb. Thus, the present data reveal a novel aspect of the potential role of a polluting metal such as Pb(II). A more detailed study based on high-resolution high-frequency EPR (290 GHz) and detailed DFT calculations on the *g*-value shift allows a more precise analysis of the radical species in humic substances and will be published in a forthcoming paper.

Acknowledgment. Y.D. has been supported through an International Greek−Polish Exchange grant by the Greek General Secretariat of Research and Technology (GGET).

Supporting Information Available: Figure S1−S3, showing FTIR and ^{13}C NMR spectra, Figure S4, showing pH titration data, Figure S5−S7, showing DFT optimized structures and spin density distribution for gallic acid−Pb and gallic acid−Mg complexes, and tables with the natural atomic charges, Mulliken atomic charges, bond overlap populations, energy calculations, and Cartesian coordinates. This material is available free of charge via the Internet at http://pubs.acs.org.

References and Notes

(1) Tipping, E. *Cation Binding by Humic Substances*, 1st ed.; Cambridge University Press: Cambridge, U.K., 2002.

(2) Stevenson, F. J. *Humus Chemsitry. Genesis, Composition, Reactions*, 2nd ed.; John Wiley and Sons: New York, 1994.
(3) McBride, M. *Environmental Chemistry of Soils*: Oxford University Press: New York, 1994.
(4) Schulten, H. R. In *Humic Substances in the Global Environment and Implications on Human Health*; Senesi, N., Miano, T. M., Eds.; Elsevier: Amsterdam, 1994.
(5) Senesi, N. *Adv. Soil Sci.* **1990**, *14*, 77.
(6) Senesi, N.; Loffredo, E. In *Soil Physical Chemistry*; Sparks D. L. Ed.; CRC Press: Boca Raton, FL, 1999; pp 239−370.
(7) Scott, D. T.; McKnight, D. M.; Blunt-Harris, E. L.; Kolesar, S. E.; Lovley, D. R.; *Environ. Sci. Technol*. **1998**, *32*, 2984.
(8) Lovley, D.; Coates, J.; Blunt-Harris, E.; Phillips, E.; Woodward, J. *Nature* **1996**, *382*, 445.
(9) Coates, J.; Ellis, D.; Blunt-Harris, E.; Gaw, C.; Roden, E.; Lovley, D. *Appl. Environ. Microbiol.* **1998**, *64*, 1504.
(10) Z. Struyk, Z.; Sposito, G. *Geoderma* **2001**, *102*, 329.
(11) Thorn, K.; Arterburn, J.; Mikita, M. *Environ. Sci. Technol.* **1992**, *26*, 107.
(12) Saiz-Jimenez, C.; Haider, K.; Martin, J. P. *Soil Sci. Soc. Am. Proc.* **1975**, *39*, 649.
(13) (a) Martin, J. P.; Haider, K.; *Soil Sci.* **1971**, *111*, 54. (b) Sonnenberg, L. B.; Johnso, J. D.; Christman, R. F. In *Aquatic Humic substances. Influence on Fate and Treatmant of Pollutants*; Suffet, I. H., MacCarthy, P., Eds.; Advances in Chemistry Series 219; American Chemical Society: Washington, DC, 1989.
(14) Jerzykiewicz, M.; Drozd, J.; Jezierski, A. *Chemosphere* **1999**, *92*, 253.
(15) Jezierski, A.; Czechowski, F.; Jerzykiewicz, M.; Golonka, I.; Drozd, J.; Byli ìnska, E.; Chen, Y.; Seaward M. R D. *Spectrochim. Acta A* **2002**, *58*, 1293.
(16) Jezierski, A.; Czechowski, F.; Jerzykiewicz, M.; Chen, Y.; Drozd, J. *Spectrochim. Acta A* **2000**, *56*, 379.
(17) Jerzykiewicz, M.; Jezierski, A.; Czechowski, F.; Drozd, J. *Org. Geochem.* **2002**, *33*, 265.
(18) Jerzykiewicz, M. *Geoderma* **2004**, *122*, 305.
(19) Alloway, B., Ed. *Heavy Metals in Soils*; Blackie Academic & Professional: Glasgow, U.K., 1995.
(20) Bourton, C. F.; Görlasch, U.; Candelone, J. P.; Bolshov, M. A.; Delams, R. J. *Nature* **1991**, *353*, 153.
(21) Manceau, A.; Boisset M.-C.; Sarret, G.; Hazemann, J.-L.; Mench, M.; Cambier, P.; Prost, R. *Environ. Sci. Technol.* **1996**, *30*, 1540.
(22) Xia, K.; Bleam, W.; Helmke, P. A. *Geochim. Cosmochim. Acta* **1997**, *61*, 2211.
(23) Yost, E. C.; Tejedor-Tejedor, M. I.; Anderson, M. A. *Environ. Sci. Technol*. **1990**, *24*, 822.
(24) Tejedor-Tejedor, M. I.; Yost, E. C.; Anderson, M. A. *Langmuir* **1992**, *8*, 525.
(25) Gu, B.; Schmitt, J.; Liang, L.; McCarthy, J. F. *Geochim. Cosmochim. Acta* **1995**, *59*, 219.
(26) Davis, J. A.; Leckie, J. O. *Environ. Sci. Technol*. **1978**, *12*, 1309.
(27) Kreller, D. I.; Gibson, G.; Novac, W.; van Loon, G. W.; Horton, J. H. *Colloids Surf., A* **2003**, *212*, 249.
(28) Ali, M. A.; Dzombak, D. A. *Geochim. Cosmochim. Acta* **1996**, *30*, 291.
(29) Banyahya, L.; Garnier, J.-M. *Environ. Sci. Technol*. **1999**, *33*, 1398.
(30) Hayes, M. H., McCarthy, P., Malcolm, R. L., Swift, R. S., Eds. *Humic Substances II: In Search of Structure*; Wiley: New York 1989.
(31) Rifaldi, R.; Schintzer, M. *Soil Sci. Soc. Am. J.* **1972**, *36*, 301.
(32) Senezi, N. *Anal. Chim. Acta* **1990**, *232*, 51.
(33) Novotny, E. H.; Martin-Neto, L. *Geoderma* **2002**, *106*, 305.
(34) Ariese, F.; van Assema, S.; Gooijer, C.; Bruccoleri, A. G.; Langford, C. H. *Aquat. Sci.* **2004**, *66*, 86.
(35) Chesire, M. V.; McPhail, D. B. *Eur. J. Soil Sci.* **1996**, *47*, 205.
(36) Wilson, S. A.; Weber, J. H. *Anal. Lett.* **1977**, *10*, 75.
(37) Eaton, D. R. *Inorg. Chem.* **1964**, *3*, 1268.
(38) Felix, C. C.; Hyde, J. S.; Sarna, T.; Sealy, R. C. *J. Am. Chem. Soc.* **1978**, *100*, 3922.
(39) Cuvelier, M.-E.; Richard, H.; Berset, C. *Biosci., Biotechnol., Biochem.* **1992**, *56*, 324.
(40) Rice-Evans, C. A.; Miller, N. J.; Paganga, G. *Free Radical Biol. Med.* **1996**, *20*, 933.
(41) Ueda, J.; Saito, N.; Shimazu, Y.; Ozawa, T. *Arch. Biochem. Biophys.* **1996**, *333*, 377.
(42) Tyrakowska, B.; Soffers, A. E. M. F.; Szymusiak, H.; Boeren, S.; Boersma, M. G.; Lemanska, K.; Vervoort, J.; Rietjens, I. M. C. M. *Free Radical Biol. Med.* **1999**, *27*, 1427.
(43) Fukumoto, L. R.; Mazza, G. *J. Agric. Food Chem.* **2000**, *48*, 3597.
(44) Schreckenbach1, G.; Ziegler, T. *Theor. Chem. Acc.* **1998**, *99*, 71.
(45) Neyman K. M.; Ganyushin D. I.; Matveev, A. V. *J. Phys. Chem. A* **2002**, *106*, 5022.
(46) Kaupp, M.; Reviakine, R.; Malkina, O. L.; Arbuznikov, A.; Schimmelpfennig, B.; Malkin, V. G. *J. Comput. Chem.* **2002**, *23*, 794.
(47) Kaupp, M.; Gress, T.; Reviakine, R.; Malkina, O. L.; Malkin, V. G. *J. Phys. Chem. B* **2003**, *107*, 331.
(48) Mohammed-Ziegler, I.; Billes, F. *J. Mol. Struct. (THEOCHEM)* **2002**, *618*, 259.
(49) Leopoldini, M.; Marino, T.; Russo, N.; Toscano, M. *J. Phys. Chem. A* **2004**, *108*, 4916.
(50) Swift, R. S. Organic Matter Characterization. *Methods of Soil Anaysis. Part 3. Chemical Methods*; Soil Science Society of America, Inc. Book Series No. 5; Madison, WI, 1996; pp 1011−1069.
(51) Hayes M. H. B. In *Humic Substances in Soil, Sediment and Water: Geochemistry, Isolation and Characterisation*; Aiken, G. R., et al., Ed.; Wiley: New York, 1985; pp 329−362.
(52) Herbelin, A. L.; Westall, J. C. *FITEQL. A Computer Program for Determination of Chemical Equilibrium Constants from Experimental Data*, Version 3.1, Report 94-01; Department of Chemistry, Oregon State University: Corvallis, OR, 1994.
(53) (a) Becke, A. D. *Phys. Rev. A.* **1988**, *38*, 3098. (b) Becke, A. D. *J. Chem. Phys.* **1992**, *96*, 215. (c) Becke, A. D. *J. Chem. Phys.* **1993**, *98*, 5648.
(54) Lee, C.; Yang, W.; Parr, R. G. *Phys. Rev. B* **1988**, *37*, 785.
(55) Dunning, T. H., Jr.; Hay, P. J. In *Modern Theoretical Chemistry*; Schaefer, H. F., III, Ed.; Plenum: New York, 1976; Vol. 3, pp 1−28.
(56) Kuechle, W.; Dolg, M.; Stoll, H.; Preuss, H. *Mol. Phys.* **1991**, *74*, 1245.
(57) Salpin, J.-Y.; Tortajada, J.; Alcami, M.; Mo, O.; Yanez, M. *Chem. Phys. Lett.* **2004**, *383*, 561.
(58) Schlegel, H. B. *J. Comput. Chem.* **1982**, *3*, 214.
(59) (a) Mulliken, R. S. *Phys. Rev.* **1932**, *41*, 66. (b) Mulliken, R. S. *J. Chem. Phys.* **1935**, *3*, 573. (c) Mulliken, R. S. *J. Chem. Phys.* **1995**, *23*, 1833, 2343, 2388.
(60) (a) Reed, A. E.; Curtiss, L. A.; Weinhold, F. *Chem. Rev.* **1988**, *88*, 899. (b) Weinhold, F. In *Encyclopedia of Computational Chemistry*; Schleyer, P. v. R., Allinger, N. L., Kollmann, P. A., Clark, T., Schaefer, H. F. S., Gasteiger, J., Schreiner, P. R., Eds.; Wiley-VCH: Chichester, U.K., 1998; Vol. 3, p 1792.
(61) Frisch, M. J.; Trucks, G. W.; Schlegel, H. B.; Scusseria, G. E.; Robb, M. A.; Cheeseman, J. R.; Zakrzewski, V. G.; Montgomery, J. A.; Vreven, T.; Kudin, K. N.; Burant, J. C.; Millan, J. M.; Iyengar, S. S.; Tomasi, J.; Barone, V.; Mennucci, B.; Cossi, M.; Scalmani, G.; Rega, N.; Petersson, G. A.; Nakatsuji, H.; Hada, M.; Ehara, M.; Toyota, K.; Fukuda. R.; Hasegawa, J.; Ishida, M.; Nakajima, T.; Honda, Y.; Kitao, O.; Nakai, H.; Klene, M.; Li, X.; Knox, J. E.; Hratchian, H. P.; Cross, J. B.; Adamo, C.; Jaramillo, J.; Gomperts, R.; Stratmann, R. E.; Yazyev, O.; Austin, A. J.; Cammi, R.; Pomelli, C.; Ochterski, J. W.; Ayala, P. Y.; Morokuma, K.; Voth, G. A.; Salvador, P.; Dannenberg, J. J.; Zakrzewski, V. G.; Dapprich, S.; Daniels, A. D.; Strain, M. C.; Farkas, O.; Malick, D. K.; Rabuck, A. D.; Raghavachari, K.; Foresman, J. B.; Ortiz, J. V.; Cui, Q.; Baboul, A. G.; Clifford, S.; Cioslowski, J.; Stefanov, B. B.; Liu, G.; Liashenko, A.; Piskorz, P.; Komaromi, I.; Martin, R. L.; Fox, D. J.; Keith, T.; Al-Laham, M. A.; Peng, C. Y.; Nanayakkara, A.; Challacombe, M.; Gill, P. M. W.; Johnson, B.; Chen, W.; Wong, M. W.; Gonzalez, C.; Pople, J. A. *Gaussian 03*, Revision B.02; Gaussian, Inc.: Pittsburgh, PA, 2003.
(62) Baes, C. F.; Mesmer, R. E. *The Hydrolysis of Cations*; Krieger: Malabar, FL, 1986; pp 358−365.
(63) Pedersen, J. A. *Handbook of ESR Spectra from Quinones and Quinols*; CRC Press: Boca Raton, FL, 1985.
(64) Wertz, J. E.; Bolton, J. R. *Electron Spin Resonance: Elementary Theory and Practical Applications*; McGraw-Hill: New York, 1972.
(65) Yoshioka, H.; Ohashi, Y.; Fukuda, H.; Senda, Y.; Yoshioka, H. *J. Phys. Chem. A* **2003**, *107*, 1127.
(66) In liquid solution sample at pH 12, the room-temperature EPR signal consists of a 1:3:1 triplet with an overall splitting of 2.4 G, similar to that previously reported,[65] for gallic acid at pH $\sim$ 12 under O_2 oxidation. This EPR triplet is characteristic of a radical interacting with two $^1H(I=1/2)$ nuclei and is assigned to the radical state of the fully deprotonated gallate anion. In accordance with reference 65, the two interacting protons are assigned to the ring protons at positions 2 and 6, which, as we show in the following by the DFT calculations, bear a small fraction of the unpaired spin density. The room-temperature EPR spectrum for pH 10.6 gallic acid sample comprises six hyperfine lines with an overall width of 4.4 G. This EPR signal is assigned to the radical state of the doubly deprotonated gallate anion. The hyperfine lines are due to four interacting ring protons at positions 2, 3, 5, and 6. The low-temperature EPR spectra that we display in Figure 3 are broader than the liquid samples because of inhomogeneous broadening and a small degree of microwave power saturation. The low-temperature EPR signals from gallic acid are saturated al low microwave power; i.e., $P_{1/2} = 2.1$ μW at 28 K, which is characteristic for isolated organic radicals with no influence by magnetic interactions;[64] in addition we have examined carefully the g 4 region for "forbidden" $\Delta m_s = 2$ transitions[64] originating from possible radical−radical interactions. In most cases we did not detect any additional EPR signal in that region. Only in cases where the samples were incubated at alkaline pH for long periods, i.e., 4 h or more, the g 2 EPR signals showed splittings accompanied by formation of g 4 "forbidden"

transitions (data not shown). Thus, at prolonged incubation times, dimeric and then polymeric species start to form from the monomeric radicals. On the contrary, the radicals presented in Figure 3, formed under short incubation period, are monomeric radicals.

(67) Inbar, Y.; Chen, Y.; Hadar, Y. *Soil. Sci. Soc. Am. J.* **1990**, *54*, 1316.

(68) Nakamoto, K. *Infrared and Raman Spectra of Inorganic and Coordination Compounds*; Wiley: New York, 1989; pp 231−247.

(69) Koll, A.; Melikova, S. M.; Karpfen, A.; Wolschann, P. *J. Mol. Struct.* **2001**, *559*, 127.

(70) Palomar, J.; De Paz, J. L. G.; Catalán, J. *Chem. Phys.* **1999**, *246*, 167.

(71) Mohammed-Ziegler, I.; Billes, F. *J. Mol. Struct. (THEOCHEM)* **2002**, *618*, 259.

(72) Vicedomini, M. *Ann. Chim.* **1987**, *77*, 789.

(73) Ohman, L.-O.; Sjoberg, S. *Acta Chem. Scand. A* **1981**, *35*, 201.

(74) Ohman, L.-O.; S. Sjoberg, S. *Acta Chem. Scand. A* **1982**, *36*, 47.

(75) Wershaw, R. L.; Llaguno, E. C.; Leenheer, J. A. *Colloids Surf., A* **1996**, *108*, 213.

(76) Bors, W.; Michel, C.; Stettmaier, K. *Arc. Biochem. Biophys.* **2000**, *374*, 347.

(77) Smith, R. M.; Martel, A. E. *Critical Stability Constants*, Vol. 3; Plenum: New York, 1989.